ORIGINAL RESEARCH

Performance of Radiomics derived morphological features for prediction of aneurysm rupture status

Calvin Gerald Ludwig , Alexandra Lauric, Justin A Malek, Ryan Mulligan, Adel M Malek

Department of Neurosurgery, Tufts Medical Center, Boston, Massachusetts, USA

Correspondence to
Dr Adel M Malek, Department of Neurosurgery, Tufts Medical Center, Boston, MA 02111, USA; amalek@tuftsmedicalcenter.org

Received 29 August 2020
Revised 6 October 2020
Accepted 9 October 2020

Check for updates

© Author(s) (or their employer(s)) 2020. No commercial re-use. See rights and permissions. Published by BMJ.

To cite: Ludwig CG, Lauric A, Malek JA, *et al*. *J NeuroIntervent Surg* Epub ahead of print: [*please include* Day Month Year]. doi:10.1136/neurintsurg-2020-016808

ABSTRACT

Background Morphological differences between ruptured and unruptured cerebral aneurysms represent a focus of neuroimaging researchfor understanding the mechanisms of aneurysmal rupture. We evaluated the performance of Radiomics derived morphological features, recently proposed for rupture status classification, against automatically measured shape and size features previously established in the literature.

Methods 353 aneurysms (123 ruptured) from three-dimensional rotational catheter angiography (3DRA) datasets were analyzed. Based on a literature review, 13 Radiomics and 13 established morphological descriptors were automatically extracted per aneurysm, and evaluated for rupture status prediction using univariate and multivariate statistical analysis, yielding an area under the curve (AUC) metric of the receiver operating characteristic.

Results Validation of overlapping descriptors for size/volume using both methods were highly correlated ($p<0.0001$, $R^2=0.99$). Univariate analysis selected AspectRatio ($p<0.0001$, AUC=0.75), Non-sphericity Index ($p<0.0001$, AUC=0.75), Height/Width ($p<0.0001$, AUC=0.73), and SizeRatio ($p<0.0001$, AUC=0.73) as best among established descriptors, and Elongation ($p<0.0001$, AUC=0.71) and Flatness ($p<0.0001$, AUC=0.72) among Radiomics features. Radiomics Elongation correlated best with established Height/Width ($R^2=0.52$), whereas Radiomics Flatness correlated best with Ellipticity Index ($R^2=0.54$). Radiomics Sphericity correlated best with Undulation Index ($R^2=0.65$). Best Radiomics performers, Elongation and Flatness, were highly correlated descriptors ($p<0.0001$, $R^2=0.75$). In multivariate analysis, established descriptors (Height/Width, SizeRatio, Ellipticity Index; AUC=0.79) outperformed Radiomics features (Elongation, Maximum3Ddiameter; AUC=0.75).

Conclusion Although recently introduced Radiomics analysis for aneurysm shape and size evaluation has the advantage of being an efficient operator independent methodology, it currently offers inferior rupture status discriminant performance compared with established descriptors. Future research is needed to extend the current Radiomics feature set to better capture aneurysm shape information.

INTRODUCTION

Higher availability and increased access to medical imaging has resulted in an increasing number of asymptomatic, unruptured cerebral aneurysms being incidentally detected during imaging investigations.[1] Once discovered, the clinical management of these aneurysms requires careful assessment, as both surgical and endovascular treatments carry age and location dependent risk of complications. Studies suggest that unruptured asymptomatic aneurysms have a relatively low risk of rupture (0.1–1.3%).[2 3] In the eventuality of rupture, however, aneurysmal subarachnoid hemorrhage carries a mortality of 40–50% and a morbidity rate of 10–20%, despite advances in management,[4] making prediction of rupture risk of high clinical value.

The exact mechanism of cerebral aneurysmal rupture is still unknown, and morphological differences between ruptured and unruptured aneurysms have been intensely studied as a way towards the understanding of the rupture phenomenon.[5] The International Study of Unruptured Intracranial Aneurysms (ISUIA) studies proposed an aneurysm size threshold between 7 and 10 mm for surgical management.[2 6] Although aneurysm size is still one of the most considered features in determining treatment options, many aneurysms rupture at sizes smaller than 7 mm.[7] Consequently, additional size and shape aneurysmal features have been considered for rupture risk determination, such as: (1) aneurysm height,[8] (2) aneurysm aspect ratio,[9] (3) height to width ratio,[10] (4) size to vessel diameter ratio,[11] (5) inflow angle,[12] and (6) shape deviations from ideal spherical or elliptical forms,[13] among others. These features have been previously evaluated on large samples of ruptured and unruptured aneurysms,[14] and are well established in the literature.

PyRadiomics (Radiomics)[15] is a recently introduced automatic imaging processing tool for pixel-by-pixel extraction of object features, including voxel intensity based and shape- based parameters. The ability of Radiomics to evaluate both shape (size, volume, sphericity, etc) as well as image characteristics, such as patterns and voxel intensity variations, has proved valuable in the study of pathological lesions. Radiomics texture descriptors were evaluated to predict prostate cancer scores with high accuracy.[16] The automated aspect of Radiomics allowed for the extractions of thousands unique per tumor features from T2 weighted imaging, diffusion weighted imaging, and T2 mapping.[16] Similarly, Radiomics texture features from T1 weighted images enabled better differentiation between glioblastoma and anaplastic oligodendroglioma,[17] as well as between glioblastoma and metastatic brain tumors.[18] Positron emission tomography Radiomics

J NeuroIntervent Surg: first published as 10.1136/neurintsurg-2020-016808 on 6 November 2020. Downloaded from http://jnis.bmj.com/ on December 25, 2020 by guest. Protected by copyright.

accurately identified the histological subtypes of lung cancer.[19] Radiomics of elastography was employed to assess liver fibrosis stages as a non-invasive diagnostic option.[20] Clearly, the ability of Radiomics to generate, in an automated fashion, a large amount of texture derived features from a variety of image modalities makes it an attractive tool for machine learning and medical informatics research.

Recent research[21 22] suggested the use of Radiomics derived features for the determination of stability of intracranial aneurysms and rupture risk stratification of cerebral aneurysms. The purpose of this study was to evaluate, in a systematic fashion, the performance of Radiomics derived morphological features against well known shape and size descriptors previously established in the literature.[9 13 14]

MATERIALS AND METHODS

Patient selection

Consecutive high resolution three-dimensional (3D) angiographic data of patients undergoing cerebral angiography were reviewed for this study. All angiographic studies with imaging of sufficient quality to permit accurate image processing and morphological analysis were included. All angiographic data for ruptured aneurysms within this set were obtained in an emergent fashion and prior to vasospasm onset. Consequently, volumetric data were available for 353 aneurysms (123 ruptured).

The research was approved by the institutional review board (IRB No 9035). Patient consent was waived because of the retrospective nature of the study not impacting patient clinical care.

Angiography and data processing

Three-dimensional catheter based cerebral angiograms (3DRA) were obtained as previously described using a calibrated biplane system,[23] with volume reconstruction using the available clinical software package, to yield a 3D volumetric dataset (figure 1A). Volumetric data sets, including aneurysm and parent vessel, were segmented using Amira 5.3 (FEI, Hillsboro, Oregon, USA).

Established size and shape feature extraction

For each segmented surface, the aneurysm dome was isolated from the surrounding vessels and represented as a 3D triangular mesh model using Amira 5.3 (figure 1A). The corresponding neck plane was defined for each aneurysm and was similarly represented as a 3D triangular mesh model. Similar to other studies in the field,[13 24] the aneurysm neck plane was selected to the best of our ability at the location where the aneurysmal sac protruded outward from the parent vessel.[23] A cross sectional plane cut was also selected on the inflow parent vessel at a distance of one vessel diameter from the aneurysmal neck (figure 1A) and was similarly represented as a triangular mesh.

Size and shape parameters were automatically extracted from the three surfaces (aneurysm, neck plane, parent vessel plane) using a previously described and validated Matlab program (V.9.8; MathWorks, Natick, Massachusetts, USA).[23] The features evaluated have been extensively used in the literature for rupture status determination (figure 1B). For the purpose of this study, we will refer to these feature groups as 'established descriptors'. They are as follows:

Aneurysm size (SizeMaximum) was defined as the largest distance between any two points on the aneurysm surface that could be fitted inside the aneurysm dome. Points that overflow the neck plane were ignored.

Aneurysm maximal height (HeightMaximum) was defined as the largest distance between the center of the neck and the aneurysm surface that could be fitted inside the aneurysm dome. This distance was not necessarily orthogonal to the neck plane. Here, the center of the neck is the centroid (geometric center) of the neck region.[23]

Aneurysm maximal width (WidthMaximum) was defined as the largest distance orthogonal to the maximal height. This is the maximum diameter along all cross sections orthogonal on the aneurysm maximal height.

Average neck size (NeckAverage) was computed as twice the average distance from the neck centroid to the neck border[23] (figure 1B).

Average parent vessel size (ParentVesselSize) was computed as twice the average distance from the parent vessel cross section centroid to the parent vessel plane border.[25]

These size features were used to evaluate (1) *the aspect ratio* (AspectRatio) as the ratio between HeightMaximum and NeckAverage, (2) *the height width* (Height/Width) as the ratio between HeightMaximum and WidthMaximum, (3) *bottleneck factor* (BottleneckFactor) as the ratio between WidthMaximum and NeckAverage, and (4) *size ratio* (SizeRatio) as the ratio between HeightMaximum and ParentVesselSize (figure 1B).

Three complex shape parameters, Non-sphericity Index (NSI), Ellipticity Index (EI), and Undulation Index (UI), were automatically evaluated using the formulas introduced by Raghavan *et al*.[13] Specifically, NSI represents the deviation of the aneurysmal shape from a sphere. The level to which an aneurysm surface deviates from a spherical shape (greater NSI) is an index of lesion instability and may indicate an increased risk of rupture.[13] UI captures the 'bumpiness' of the aneurysm wall (irregularities, lobulations, or daughter sacs). The greater the undulation of the surface, the greater the UI value. Finally, EI describe the ellipticity of an aneurysm. EI varies from 0 to 1 and is equal to 0 for a hemisphere and increases with increasing ellipticity. EI is higher for both egg shaped and mushroom shaped aneurysms.

PyRadiomics morphological feature extraction

PyRadiomics package, implemented in Python, was used.[15] Because image intensity derived features are not relevant to angiographic morphology analysis, only shape parameters were included in the analysis, similar to previous work.[21] For the purpose of this study, we will refer to this feature group as 'Radiomics descriptors'. Aneurysmal surfaces were voxelized using a Matlab script such that mesh surfaces were represented as a DICOM volume, which represented the input to PyRadiomics. All available Radiomics morphological descriptors were extracted: SurfaceArea (the total area of the shape), MeshVolume (the total volume of the shape), SurfaceVolumeRatio (the ratio of surface area to volume of a shape), Sphericity (a measure of how close the shape resemble a sphere), Maximum3DDiameter (the largest pairwise Euclidean distance between any surface mesh vertices), Maximum2DDiameterSlice (the largest pairwise Euclidean distance between surface mesh vertices in the axial plane), Maximum2DDiameterColumn (the largest pairwise Euclidean distance between surface mesh vertices in coronal plane), Maximum2DDiameterRow (the largest pairwise Euclidean distance between surface mesh vertices in the sagittal plane), MajorAxisLength (the largest axis length of the enclosing ellipsoid), MinorAxisLength (the second largest axis length of the enclosing ellipsoid), LeastAxisLength (the smallest axis length of the enclosing ellipsoid), Elongation (a measure of the relationship between the two largest principal components in the shape) is defined as the ratio MinorAxisLength/MajorAxisLength, and Flatness (a measure of the relationship between the largest and smallest principal components in the

J NeuroIntervent Surg: first published as 10.1136/neurintsurg-2020-016808 on 6 November 2020. Downloaded from http://jnis.bmj.com/ on December 25, 2020 by guest. Protected by copyright.

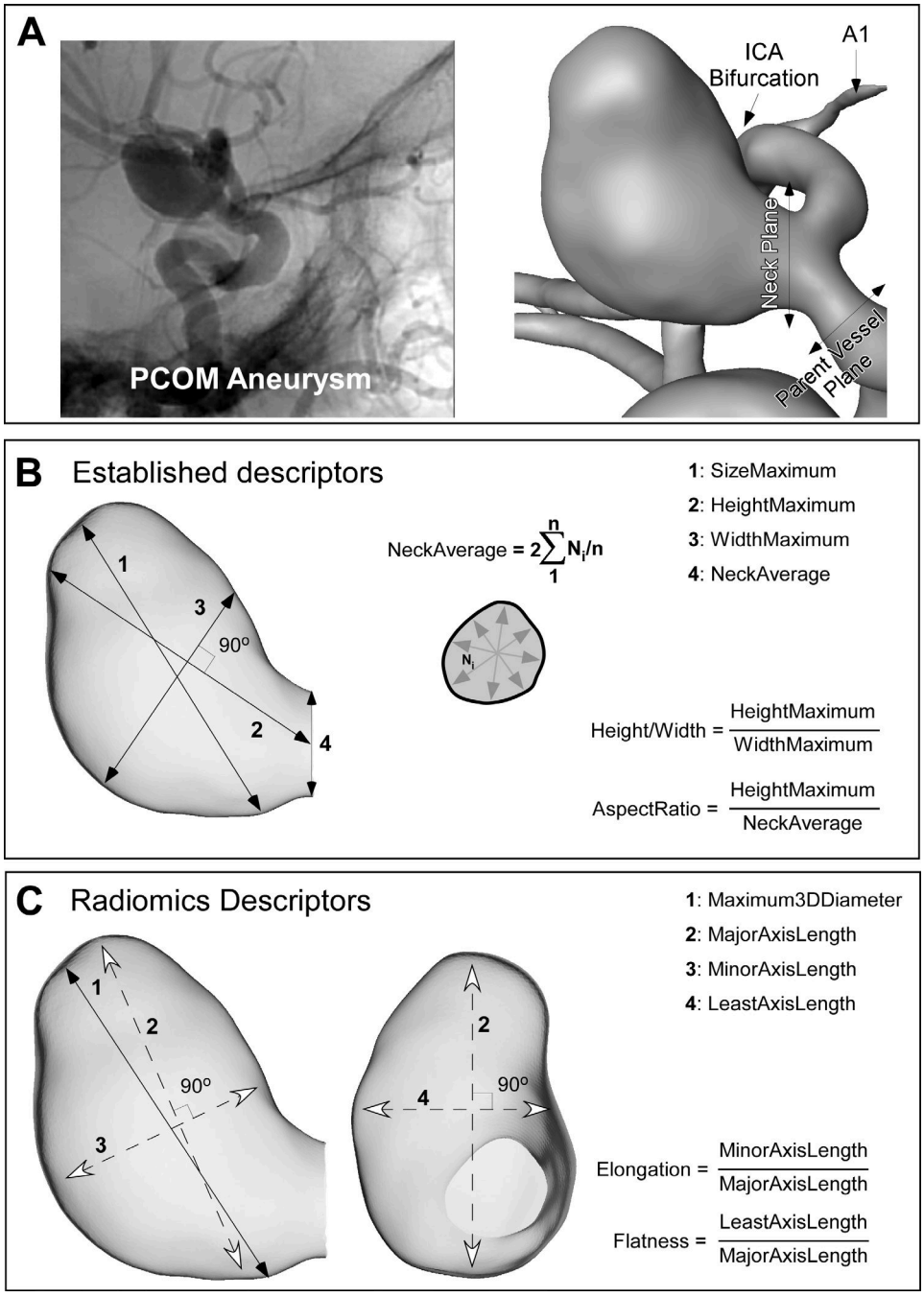


Figure 1 (A) Three-dimensional volumetric rendering of three-dimensional rotational catheter angiography and segmentation of the vascular structure from surrounding tissue and representation of the surface as a triangular mesh. (B) Evaluation of established descriptors. Neck plane is shown as a thin horizontal line. SizeMaximum is the maximal diameter of the dome. HeightMaximum is the maximal distance from the neck center to the aneurysm dome. WidthMaximum is the maximal distance orthogonal to WeightMaximum. NeckAverage is computed as twice the average distance from the neck center to the neck border. (C) Evaluation of Radiomics descriptors. Maximum3DDiameter is the largest pairwise Euclidean distance between any surface mesh vertices. MajorAxisLength, MinorAxisLength, and LeastAxisLength are computed from the principal component analysis of the three-dimensional voxel set. ICA, internal carotid artery; PCOM, posterior communicating artery.

shape) is defined as the ratio LeastAxisLength/MajorAxisLength (figure 1C). The three axes of the shape (MajorAxisLength, MinorAxisLength, and LeastAxisLength) are computed using principal component analysis, using the physical coordinates of each voxel, taking voxel size into account, but not the shape mesh. Detailed information of these features is available in the documentation for PyRadiomics (http://PyRadiomics.readthedocs.io/en/latest/).

Statistical analysis

JMP statistical software (V.Pro 14, SAS Institute, Cary, North Carolina, USA) was used to evaluate the performance of all parameters in discriminating ruptured status. Statistical significance was assumed for $p<0.05$. All variables were tested independently using the Student's t test analysis. Receiver operating characteristics (ROC) curve was performed and prediction accuracy was evaluated using the area under the curve (AUC)

J NeuroIntervent Surg: first published as 10.1136/neurintsurg-2020-016808 on 6 November 2020. Downloaded from http://jnis.bmj.com/ on December 25, 2020 by guest. Protected by copyright.

index. Multivariate statistical analysis was evaluated using stepwise forward feature selection of size, shape, and Radiomics parameters for rupture status discrimination. Only those parameters that were statistically significant in the univariate analysis ($p<0.05$) were included in the multivariate analysis.

RESULTS

Patient demographics

A total of 353 3D rotational angiographic volumes representing cerebral aneurysms were analyzed for this study. The distribution of aneurysms by location was as follows: 95 anterior communicating artery, 60 middle cerebral artery, 52 internal carotid artery, 51 posterior communicating artery, 24 basilar artery, 24 ophthalmic artery, 17 internal carotid artery bifurcation, 10 anterior choroidal artery, 6 superior cerebellar artery, 5 anterior cerebral artery, 4 vertebral artery, 3 posterior inferior cerebellar artery, and 2 posterior cerebral artery. There were 230 unruptured aneurysms (181 women; 56.62±13.49 years) and 123 ruptured aneurysms (80 women; 56.01±15.94 years). There was no statistically significant difference in age between the ruptured and unruptured subgroups ($p=0.71$).

Correlation between established and Radiomics descriptors

In order to describe the relationships between established and Radiomics descriptors, statistical correlations were evaluated between the two feature sets (figure 2, top row) to serve as cross validation. There was perfect correlation between Size-Maximum and Maximum3Ddiameter ($p<0.0001$, $R^2=0.99$), between established Volume and Radiomics MeshVolume ($p<0.0001$, $R^2=0.99$), and between established Area and Radiomics SurfaceArea ($p<0.0001$, $R^2=0.99$).

Radiomics Elongation correlated best with established Height/Width ($p<0.0001$, $R^2=0.52$), followed by EI ($p<0.0001$, $R^2=0.38$) and NSI ($p<0.0001$, $R^2=0.35$) in decreasing order (figure 2, second row). Similarly, Radiomics Flatness correlated best with EI ($p<0.0001$, $R^2=0.54$), followed by NSI ($p<0.0001$, $R^2=0.44$) and Height/Width ($p<0.0001$, $R^2=0.39$) (figure 2, third row). Radiomics Sphericity correlated best with UI ($p<0.0001$, $R^2=0.65$), followed by EI ($p<0.0001$, $R^2=0.45$) and least with established NSI ($p<0.0001$, $R^2=0.38$) (figure 2, bottom row).

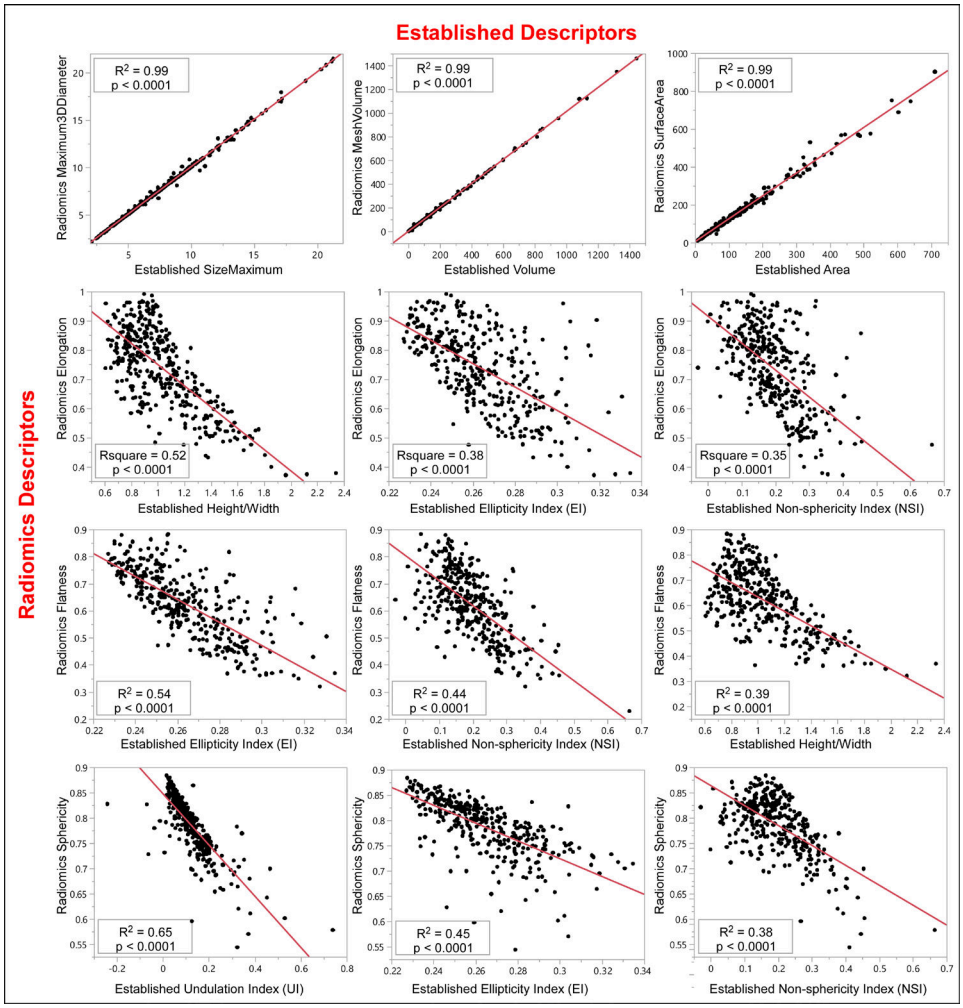


Figure 2 (Top row) Correlation between pairs of overlapping features from the Radiomics and established set: Maximum3DDiameter–SizeMaximum; MeshVolume–Volume; and SurfaceArea–Area. (Second row) Correlation between Radiomics Elongation and established parameters. Shown are the three strongest correlations in decreasing order: Height/Width, Ellipticity Index, and Non-sphericity. (Third row) Correlation between Radiomics Flatness and established parameters. Shown are the three strongest correlations in decreasing order: Ellipticity Index, Non-sphericity, and Height/Width. (Bottom row) Correlation between Radiomics Sphericity and established parameters. Shown are the three strongest correlations in decreasing order: Undulation Index, Ellipticity Index, and Non-sphericity.

J NeuroIntervent Surg: first published as 10.1136/neurintsurg-2020-016808 on 6 November 2020. Downloaded from http://jnis.bmj.com/ on December 25, 2020 by guest. Protected by copyright.

Table 1 Univariate statistical analysis of established size, shape, and newly introduced Radiomics parameters for rupture status discrimination

Parameter	Aneurysms Unruptured (n=230)	Aneurysms Ruptured (n=123)	P value	AUC
Age (years)	56.62±13.49	56.01±15.94	0.71	0.51
Established size and shape descriptors				
SizeMaximum (mm)	6.98±3.04	8.6±3.9	<0.0001*	0.63
NeckAverage (mm)	4.02±1.39	3.82±1.4	0.1925	0.55
Area (mm^2)	97.09±91.77	134.79±131.82	0.002*	0.59
Volume (mm^3)	113.44±162.65	168.84±246.89	0.012*	0.56
HeightMaximum (mm)	5.41±2.64	7.09±3.43	<0.0001*	0.65
WidthMaximum (mm)	5.63±2.4	6.11±2.8	0.0885	0.54
Height/Width	0.96±0.22	1.19±0.31	<0.0001*	0.73
AspectRatio	1.36±0.53	1.92±0.82	<0.0001*	0.75
BottleneckFactor	1.52±0.4	1.86±0.62	<0.0001*	0.68
SizeRatio	1.94±1.09	2.98±1.55	<0.0001*	0.73
Non-sphericity Index	0.17±0.09	0.24±0.07	<0.0001*	0.75
Ellipticity Index	0.26±0.02	0.27±0.02	<0.0001*	0.66
Undulation Index	0.11±0.08	0.14±0.09	0.0003*	0.66
Radiomics descriptors				
Elongation	0.77±0.12	0.67±0.14	<0.0001*	0.71
Flatness	0.65±0.12	0.56±0.12	<0.0001*	0.72
LeastAxisLength (mm)	3.89±1.65	4.17±1.91	0.1501	0.53
MajorAxisLength (mm)	6.11±2.81	7.64±3.65	<0.0001*	0.63
Maximum2DDiameterColumn (mm)	6.24±2.71	7.45±3.57	0.0004*	0.60
Maximum2DDiameterRow (mm)	6.34±2.75	7.31±3.45	0.0044*	0.57
Maximum2DDiameterSlice (mm)	6.33±2.78	7.25±3.21	0.0053*	0.59
Maximum3DDiameter (mm)	7.08±3.09	8.67±3.93	<0.0001*	0.62
MeshVolume (mm^3)	116.71±166.07	169.51±249.75	0.018*	0.56
MinorAxisLength (mm)	4.59±1.95	4.95±2.25	0.1148	0.54
Sphericity	0.79±0.06	0.77±0.06	0.0004*	0.65
SurfaceArea (mm^2)	127.73±124.43	164.42±157.93	0.0169*	0.57
SurfaceVolumeRatio(1/mm)	1.77±0.83	1.64±0.73	0.1441	0.54

Values are mean±SD.
*Indicates statistical significance (assumed for p<0.05).
AUC, area under the receiver operating characteristic curve.

Univariate statistical analysis

As shown in table 1, all established size and shape parameters, except for NeckAverage and WidthMaximum, were statistically significant in predicting rupture status. Although ruptured aneurysms were significantly larger compared with unruptured aneurysms (8.6±3.9 mm vs 6.98±3.04 mm, p<0.0001), maximal size (AUC=0.63) performed weakly in rupture status prediction. AspectRatio (p<0.0001, AUC=0.75), NSI (p<0.0001, AUC=0.75), Height/Width (p<0.0001, AUC=0.73), and SizeRatio (p<0.0001, AUC=0.73) were identified as the best among established parameters for rupture status classification in the univariate analysis. Ruptured aneurysms had a significantly larger aspect ratio (1.92±0.82 vs 1.36±0.53), greater height/width (1.19±0.31 vs 0.96±0.22), higher NSI (0.24±0.07 vs 0.17±0.09), and higher size ratio (2.98±1.55 vs 1.94±1.09) compared with unruptured aneurysms (figure 3A).

Similarly, most Radiomics parameters were statistically significant in predicting rupture status (table 1). Elongation (p<0.0001, AUC=0.71), and Flatness (p<0.0001, AUC=0.72) were identified as the most important Radiomics features for status prediction. Ruptured aneurysms had significantly lower Elongation (0.67±0.14 vs 0.77±0.12) and lower Flatness (0.56±0.12 vs 0.65±0.12) compared with unruptured aneurysms.

Multivariate statistical analysis

Multivariate statistical analysis was evaluated using stepwise forward feature selection of size, shape, and Radiomics parameters for rupture status discrimination (figure 3B). Only those parameters that were statistically significant in the univariate analysis were included in the multivariate analysis. From the established group, Height/Width (p=0.003), SizeRatio (p<0.0001), and EI (p=0.03) were stepwise selected for multivariate analysis (AUC=0.79) (figure 3C). From the Radiomics group, Elongation (p<0.0001), Maximum3DDiameter (p=0.003), and MajorAxisLength (p=0.008) were selected in a forward stepwise fashion for multivariate analysis (AUC=0.75). For both sets for features, adding additional descriptors to the multivariate set did not result in improved statistical performance.

J NeuroIntervent Surg: first published as 10.1136/neurintsurg-2020-016808 on 6 November 2020. Downloaded from http://jnis.bmj.com/ on December 25, 2020 by guest. Protected by copyright.

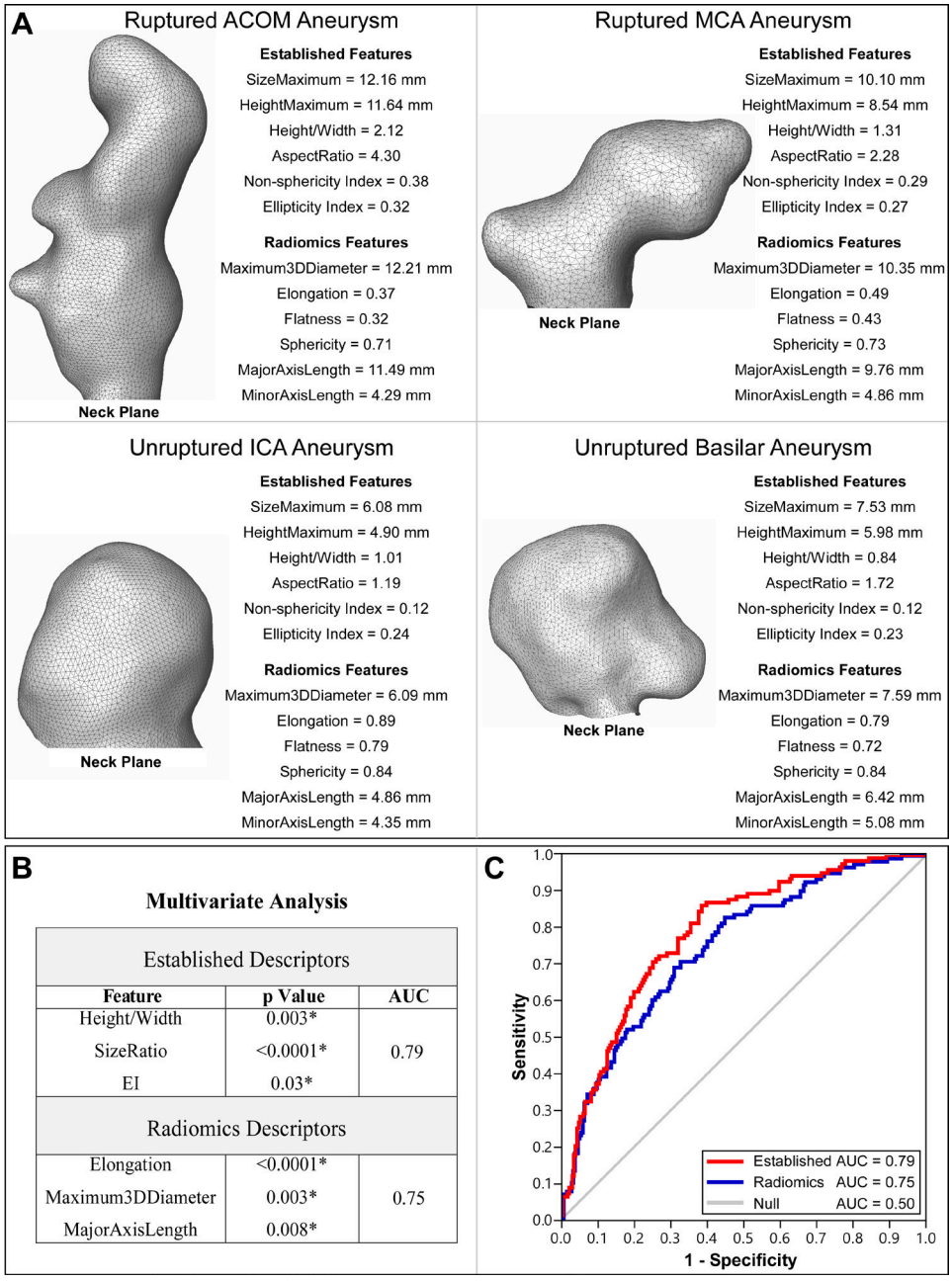


Figure 3 (A) Established and Radiomics features for four sample aneurysms: a ruptured anterior communicating artery (ACOM) aneurysm, a ruptured middle cerebral artery (MCA) aneurysm, an unruptured internal carotid artery (ICA) aneurysm, and an unruptured basilar aneurysm. (B) Multivariate analysis of established and Radiomics descriptors. Statistical significance was assumed for $p<0.05$. AUC indicates the area under the receiver operating characteristics curve (ROC) curve. (C) ROC curves for the established and Radiomics feature sets.

Elongation and Flatness were dependent variables ($p<0.0001$, $R^2=0.75$), and although they were the best Radiomics performers, there was no added value in using both features in the multivariate analysis.

DISCUSSION

Because Radiomics derived features capture both morphological and imaging characteristics, they have been used in the study of various types of pathological lesions[16–20] and, more recently,[21 22] for rupture status prediction of cerebral aneurysms. Liu *et al*[21] used Radiomics derived morphological features for prediction of aneurysm stability and described Flatness as the most important predictor with an AUC of 0.73. Zhang *et al*[22] reported Radiomics Elongation as a predictor for angiographic occlusion status post flow diverter embolization of cerebral aneurysms.

One clear advantage of using Radiomics for aneurysm feature evaluation is the convenience of single platform use (such as 3D Slicer[26]) for the entire pipeline of image processing, segmentation, and feature measurement. It should be noted, however, that in the case of cerebral aneurysms, the use of imaging contrast during data acquisition renders the Radiomics grayscale image characteristics irrelevant and only morphological features are considered.[21 22] Consequently, this study compares the aneurysmal rupture status prediction performance of 13 established size and shape descriptors to that of 13 Radiomics derived size and shape features. Similar to Radiomics features, the established

J NeuroIntervent Surg: first published as 10.1136/neurintsurg-2020-016808 on 6 November 2020. Downloaded from http://jnis.bmj.com/ on December 25, 2020 by guest. Protected by copyright.

parameters were automatically evaluated using a tool previously validated.[23] Indeed, pairs of overlapping features (maximal size, volume, and surface area) from the two feature sets showed almost perfect statistical correlation, providing validation for the two methods (figure 2).

Overall, our results showed that Radiomics derived Elongation and Flatness were the best predictors of rupture status with AUC values of 0.71 and 0.72, respectively, consistent with the results from Liu *et al*.[21] However, several established parameters, such as AspectRatio (AUC=0.75), NSI (AUC=0.75), Height/Width (AUC=0.73), and SizeRatio (AUC=0.73), outperformed Radiomics for rupture status discrimination. Similarly, in multivariate analysis, established descriptors (AUC=0.79) outperformed Radiomics features (AUC=0.75).

In terms of dependence between established and Radiomics features, Elongation was negatively correlated with Height/Width, EI, and NSI, in decreasing order of correlation strength (figure 2). In turn, Flatness was negatively correlated with EI, Height/Width, and UI, in decreasing order of correlation strength. Moreover, Elongation and Flatness were closely dependent (R^2=0.75) and pairing them in multivariate analysis had no added rupture discrimination predictive power. Paradoxically, Radiomics Sphericity was better correlated with UI and EI, but not with the established NSI, highlighting the differences between the two feature sets. One possible reason is the fact that Radiomics incorporates neck area as part of the aneurysm surface, in contrast with established methods.

While one platform processing is an advantage, Radiomics does not reveal the orientation of the aneurysm. In addition, it provides no information regarding the neck of the aneurysms. Whereas Radiomics Elongation and Flatness help in identifying the overall proportion of an aneurysm (as does the established EI), only estimation of aneurysm height provides the direction of the deformation (egg shaped or mushroom shaped aneurysm). Height characteristics influence the aneurysm hemodynamics, and were strongly correlated with surface wall shear stress,[27] a feature previously associated with aneurysmal risk of rupture.[28]

Whereas the current study showed that Radiomics performance for rupture status discrimination is not superior to that of established features in a standalone analysis, we believe Radiomics analysis has the potential to become a tool of interest in aneurysm research. Podgorsak *et al*[29] has described a method for automatic Radiomics feature extraction for angiographic parametric imaging analysis of intracranial aneurysms. Radiomics descriptors were used as biomarkers related to the contrast of blood flow in the aneurysmal sac. Similarly, automatic extraction of angiographic parametric imaging Radiomics features were investigated for the prediction of intracranial aneurysm occlusion pre- and post-intervention.[30] Although angiographic imaging is typically used to evaluate the morphological structure of neurovascular disease, such as intracranial aneurysms, stenosis, or arteriovenous malformations, the addition of angiographic parametric imaging Radiomics features allows also for the evaluation of the functional nature of these lesions. Neurointerventionalists may find it useful for evaluating the disease, predicting progression, and procedure planning.

Study limitations

This study was not a prospective evaluation of aneurysmal rupture risk based on Radiomics or established predictors of rupture, but rather a retrospective analysis of the accuracy in rupture status discrimination. As with similar retrospective research, the association between rupture status and aneurysm morphology suggested a correlation, but did not demonstrate causation. This is a limitation shared with all similar research.

The established and Radiomics features were evaluated as two separate sets. This study did not combine the two sets, and did not evaluate the incremental value of Radiomics parameters when added to established features. This analysis will be the topic of future research studies.

CONCLUSION

Recently introduced Radiomics derived parameters were proposed for aneurysm ruptured status prediction. The Radiomics Elongation and Flatness features were the best performers of the feature group, with AUC values of 0.71 and 0.72, respectively. Established size and shape parameters, such as aspect ratio, height/width, NSI, and size ratio all outperformed Radiomics descriptors, both in univariate (AUC=0.75) and multivariate analyses (AUC=0.79). Radiomics feature extraction has the advantage of being a one step, operator independent methodology. However, it currently offers relatively inferior rupture status discriminant performance compared with established descriptors. Future research is needed to extend the current Radiomics descriptors to better capture aneurysm shape information.

Twitter Calvin Gerald Ludwig @calvin__ludwig

Contributors All authors are justifiably credited with authorship according to the authorship criteria. CGL: acquisition of the data, image processing, data analysis, and editing of the manuscript. AL: acquisition of the data, image processing, analysis and interpretation of the data, and drafting of the manuscript. JAM: acquisition of the data. RM: acquisition of the data. AMM: conception, design, acquisition of the data, analysis and interpretation of the data, critical revision, and final approval.

Funding The authors have not declared a specific grant for this research from any funding agency in the public, commercial, or not-for-profit sectors.

Competing interests None declared.

Patient consent for publication Not required.

Ethics approval This research was approved by Tufts Health Sciences Campus institutional review board (IRB No 9035). Patient consent was waived because of the retrospective nature of the study not impacting patient clinical care.

Provenance and peer review Not commissioned; externally peer reviewed.

Data availability statement Data are available upon reasonable request. Data are available upon reasonable request. Study data are from Tufts Medical Center clinical imaging repository, and as such contain patient identification, and cannot be shared in their raw state. De-identified models may be available upon reasonable request.

ORCID iDs
Calvin Gerald Ludwig http://orcid.org/0000-0002-1938-4273
Adel M Malek http://orcid.org/0000-0002-0642-7609

REFERENCES

1 Vernooij MW, Ikram MA, Tanghe HL, *et al*. Incidental findings on brain MRI in the general population. *N Engl J Med* 2007;357:1821–8.
2 International Study of Unruptured Intracranial Aneurysms Investigators. Unruptured intracranial aneurysms--risk of rupture and risks of surgical intervention. *N Engl J Med* 1998;339:1725–33.
3 Juvela S, Porras M, Poussa K. Natural history of unruptured intracranial aneurysms: probability of and risk factors for aneurysm rupture. *J Neurosurg* 2000;93:379–87.
4 van Gijn J, Kerr RS, Rinkel GJE. Subarachnoid haemorrhage. *Lancet* 2007;369:306–18.
5 Sforza DM, Putman CM, Cebral JR. Hemodynamics of cerebral aneurysms. *Annu Rev Fluid Mech* 2009;41:91–107.
6 Wiebers DO, Whisnant JP, O'Fallon WM. The natural history of unruptured intracranial aneurysms. *N Engl J Med* 1981;304:696–8.
7 AlMatter M, Bhogal P, Aguilar Pérez M, *et al*. The size of ruptured intracranial aneurysms: a 10-year series from a single center. *Clin Neuroradiol* 2019;29:125–33.
8 Mocco J, Brown RD, Torner JC, *et al*. Aneurysm morphology and prediction of rupture: an international study of unruptured intracranial aneurysms analysis. *Neurosurgery* 2018;82:491–6.
9 Ujiie H, Tamano Y, Sasaki K, *et al*. Is the aspect ratio a reliable index for predicting the rupture of a saccular aneurysm? *Neurosurgery* 2001;48:495–503.

J NeuroIntervent Surg: first published as 10.1136/neurintsurg-2020-016808 on 6 November 2020. Downloaded from http://jnis.bmj.com/ on December 25, 2020 by guest. Protected by copyright.

10 Hoh BL, Sistrom CL, Firment CS, *et al*. Bottleneck factor and height-width ratio: association with ruptured aneurysms in patients with multiple cerebral aneurysms. *Neurosurgery* 2007;61:716–23.
11 Rahman M, Smietana J, Hauck E, *et al*. Size ratio correlates with intracranial aneurysm rupture status. *Stroke* 2010;41:916–20.
12 Baharoglu M, Schirmer C, Hoit D, *et al*. Aneurysm inflow-angle as a discriminant for rupture in sidewall cerebral aneurysms: morphometric and computational fluid dynamic analysis. *Stroke; a journal of cerebral circulation* 2010;41:1423–30.
13 Raghavan ML, Ma B, Harbaugh RE. Quantified aneurysm shape and rupture risk. *J Neurosurg* 2005;102:355–62.
14 Baharoglu MI, Lauric A, Gao B-L, *et al*. Identification of a dichotomy in morphological predictors of rupture status between sidewall- and bifurcation-type intracranial aneurysms. *J Neurosurg* 2012;116:871–81.
15 van Griethuysen JJM, Fedorov A, Parmar C, *et al*. Computational Radiomics system to decode the radiographic phenotype. *Cancer Res* 2017;77:e104–7.
16 Toivonen J, Montoya Perez I, Movahedi P, *et al*. Radiomics and machine learning of multisequence multiparametric prostate MRI: towards improved non-invasive prostate cancer characterization. *PLoS One* 2019;14:e0217702.
17 Fan Y, Chen C, Zhao F, *et al*. Radiomics-based machine learning technology enables better differentiation between glioblastoma and anaplastic oligodendroglioma. *Front Oncol* 2019;9:1164.
18 Chen C, Ou X, Wang J, *et al*. Radiomics-based machine learning in differentiation between glioblastoma and metastatic brain tumors. *Front Oncol* 2019;9:806.
19 Hyun SH, Ahn MS, Koh YW, *et al*. A machine-learning approach using PET-based Radiomics to predict the histological subtypes of lung cancer. *Clin Nucl Med* 2019;44:956–60.
20 Wang K, Lu X, Zhou H, *et al*. Deep learning Radiomics of shear wave elastography significantly improved diagnostic performance for assessing liver fibrosis in chronic hepatitis B: a prospective multicentre study. *Gut* 2019;68:729–41.
21 Liu Q, Jiang P, Jiang Y, *et al*. Prediction of aneurysm stability using a machine learning model based on PyRadiomics-derived morphological features. *Stroke* 2019;50:2314–21.
22 Zhang Y, Ma C, Liang S, *et al*. Morphologic feature elongation can predict occlusion status following pipeline embolization of intracranial aneurysms. *World Neurosurg* 2018;119:e934–40.
23 Lauric A, Baharoglu MI, Malek AM. Ruptured status discrimination performance of aspect ratio, height/width, and bottleneck factor is highly dependent on aneurysm sizing methodology. *Neurosurgery* 2012;71:38–46.
24 Xiang J, Natarajan SK, Tremmel M, *et al*. Hemodynamic–morphologic discriminants for intracranial aneurysm rupture. *Stroke* 2011;42:144–52.
25 Dhar S, Tremmel M, Mocco J, *et al*. Morphology parameters for intracranial aneurysm rupture risk assessment. *Neurosurgery* 2008;63:185–97.
26 Kikinis R, Pieper SD, Vosburgh KG. 3D Slicer: a platform for subject-specific image analysis, visualization, and clinical support. In: Jolesz FA, ed. *Intraoperative imaging and image-guided therapy*. New York, NY: Springer New York, 2014: 277–89.
27 Qiu T-L, Jin G-L, Bao W-Q, *et al*. Morphological effect on wall shear stress in intracranial aneurysms. *J Neurol Surg A Cent Eur Neurosurg* 2018;79:108–15.
28 Lauric A, Hippelheuser J, Cohen AD, *et al*. Wall shear stress association with rupture status in volume matched sidewall aneurysms. *J Neurointerv Surg* 2014;6:466–73.
29 Podgorsak AR, Rava RA, Shiraz Bhurwani MM, *et al*. Automatic radiomic feature extraction using deep learning for angiographic parametric imaging of intracranial aneurysms. *J Neurointerv Surg* 2020;12:417–21.
30 Shiraz Bhurwani MM, Waqas M, Podgorsak AR, *et al*. Feasibility study for use of angiographic parametric imaging and deep neural networks for intracranial aneurysm occlusion prediction. *J Neurointerv Surg* 2020;12:714–9.

J NeuroIntervent Surg: first published as 10.1136/neurintsurg-2020-016808 on 6 November 2020. Downloaded from http://jnis.bmj.com/ on December 25, 2020 by guest. Protected by copyright.